ACS Catalysis

Research Article

pubs.acs.org/acscatalysis

Tuning the Pore Structure and Surface Properties of Carbon-Based Acid Catalysts for Liquid-Phase Reactions

Isao Ogino,* Yukei Suzuki, and Shin R. Mukai

Division of Applied Chemistry, Graduate School of Engineering, Hokkaido University, Sapporo, Hokkaido 060-8628, Japan

Supporting Information

ABSTRACT: A series of sulfonic-acid-containing carbon catalysts were synthesized through the pyrolyzation of resorcinol−formaldehyde resins and subsequent sulfonation to investigate the tunability of their pore structure and surface properties. These catalysts were characterized by nitrogen gas adsorption, water vapor adsorption, elemental analysis, Boehm titration, and IR spectroscopy. Catalytic consequences of these properties were examined using two esterification reactions in which reactants of substantially different sizes (oleic acid vs acetic acid) are involved as well as the condensation of furfural with 2-methylfuran. The esterification of acetic acid with ethanol proceeded at nearly the same activity (TOF ∼ 0.02 s^{-1}) for all synthesized catalysts regardless of the variation of their surface and pore properties. Poisoning experiments of acid groups in the synthesized catalysts with NaCl indicate that nearly all $-SO_3H$ groups are accessible to the reactants. However, the esterification of oleic acid with methanol requires a large volume of mesopores (>0.4 cm^3 g^{-1}) to proceed as efficiently as that using *p*-toluenesulfonic acid (*p*-TSA) as the catalyst. The condensation reaction requires both hydrophobic surfaces and a large volume of mesopores. A synthesized carbon-based catalyst having a large mesopore volume (1.1 cm^3 g^{-1}) and surfaces with a relatively high hydrophobicity catalyzes this reaction at a much higher rate and higher selectivity (>90%) than Amberlyst-15. The results reported here show that the pore structure and surface properties of phenolic-resin-derived carbon catalysts can be easily tuned to maximize their catalytic performance in the reaction for which they are intended.

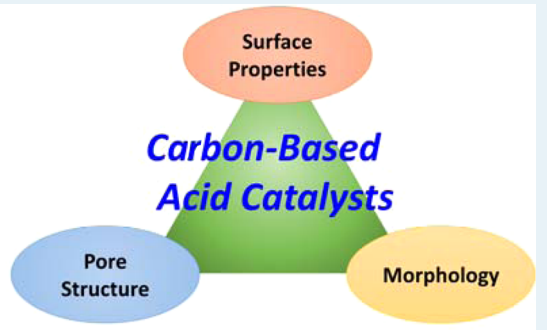

KEYWORDS: *solid acid catalyst, carbon, mesoporous, esterification, condensation, oleic acid, furfural*

INTRODUCTION

Solid acid catalysts are advantageous over liquid acids because they are noncorrosive, easier to handle and recycle, cause less waste disposal problems, and enable the use of continuous-flow processes. Among various types of solid acid catalysts,[1−20] carbon-based acid catalysts[9−20] are appealing for liquid-phase reactions because carbons are generally resistant to acidic and basic media often required in these reactions. In particular, sulfonic-acid-containing carbon catalysts derived from pyrolysis of sugars at relatively low temperatures (673−773 K) have proved their high performance in various liquid-phase reactions, particularly those involving polar substrates.[9−13,18] These catalysts have low surface areas in the dry form (BET surface area <5 m^2 g^{-1} as measured by nitrogen gas adsorption technique). However, when these catalysts are used in a reaction media that is highly polar, the catalyst particles swell and the accessibility to the acid sites within them is facilitated. However, it remains challenging to use these catalysts in a reaction media containing large and hydrophobic reactants.[14] Thus, to broaden the range of reactions that carbon-based acid catalysts can catalyze efficiently, we aimed to synthesize carbon-based acid catalysts whose pore structure and surface properties can be readily tailored. To achieve this goal, we chose carbon materials derived from the pyrolysis of resorcinol−formaldehyde (RF) resins.[21−24] These carbons are appealing from several points of view: their surface properties can be varied from hydrophilic to hydrophobic while maintaining highly porous structures[25] to meet goals of each reaction; they possess three-dimensional pore architectures with through-connected mesopores, which minimizes blockage of pores and consequently enables facile mass transport like other aerogel materials;[26] their pore structures can be varied over a wide range (micromeso-macro) via synthesis conditions of precursor resins; ultrahigh surface area carbons (∼3000 m^2 g^{-1}) with a large mesopore volume can be synthesized through physical activation using CO_2 gas;[27,28] monolithic carbons having honeycomb structure (denoted as carbon microhoneycomb, CMH), which is suitable for applications to a continuous-flow reaction system, can be readily prepared by applying the ice templating method to the sol−gel synthesis of precursor resins.[25,29−33] Relative ease of morphology control of resin-derived carbons is an important feature particularly for applications of carbon-based catalysts to a continuous-flow reaction system because the economical operation of a packed bed reactor is often limited by pressure drop through the bed,[34] and moreover, it is generally more difficult to pelletize carbon

Received: May 15, 2015
Revised: July 11, 2015
Published: July 13, 2015

DOI: 10.1021/acscatal.5b01022
ACS Catal. 2015, 5, 4951−4958

materials than metal oxides.[35] Our previous work demonstrated that a sulfonic-acid-containing CMH (CMH−SO_3H) exhibits a significantly low hydraulic resistance to a liquid flow and a stable catalytic performance in the esterification reaction of acetic acid with ethanol.[36]

Here, we show that we can tailor the surface properties (hydrophobicity) and pore structure of sulfonic-acid-containing carbon catalysts by two key synthesis parameters: resorcinol/base catalyst molar ratio in the precursor RF resin synthesis and pyrolyzation temperature. Our focus here is to tailor the properties of CMH−SO_3H for future applications of these catalysts to continuous-flow reaction systems, but the results should be applicable to other RF resin-based carbons because of the similarity in their synthesis methods.

We examined the catalytic performance of the synthesized catalysts in several liquid-phase reactions: esterification reactions of acetic acid with ethanol and oleic acid with methanol, and a condensation reaction of furanic compounds (furfural and 2-methylfuran). The two esterification reactions employ substrates with substantially different size and hydrophobicity (acetic acid vs oleic acid), and the condensation reaction employs hydrophobic furanic substrates,[37−40] forming a large nm-sized product (2,2′-(2-furylmethylene)bis(5-methylfuran), **1**). All of the reactions are technologically important classes of reactions. Liquid-phase esterification of carboxylic acids with alcohols and transesterification of esters with alcohols are often used to produce emulsifiers, fuels, and precursors for flavors, pharmaceuticals, plasticizers. A number of solid acid catalysts such as macroreticular cation-exchange resins (e.g., Amberlyst-15),[2,3,7,41] Nafion resins,[42] niobic acid, Cs-exchanged heteropoly acids,[4] sulfated zirconia, zeolites[6] are known to catalyze such reactions. Data reported for sulfonic-acid-containing solid catalysts give the benchmark to evaluate the catalysts synthesized in the current work. Condensation reactions of furanic compounds such as 2-methylfuran with an aldehyde through electrophilic aromatic substitution have been proposed to synthesize biodiesel precursors.[37,39,40] Solid acid catalysts that have a high external surface area and/or hydrophobic surfaces are reported to catalyze these reactions effectively. In this work, we chose the reaction of 2-methylfuran with furfural to form **1** to examine how the pore structure and surface properties of synthesized catalysts affect their catalytic properties. The reactions were conducted first in a batch reactor using a crushed CMH−SO_3H catalyst to evaluate the effects of the pore structure and surface properties of the catalysts on catalytic performance, and accessibility of substrates to active sites. Then, the condensation reaction was also performed in a continuous flow using CMH−SO_3H in the monolith form.

We show that the esterification of acetic acid with ethanol proceeds at similar turnover frequencies (TOFs, per −SO_3H group) regardless of the surface properties and pore structure of CMH−SO_3H catalysts because of easy access of these reactants to all acid sites. However, the esterification reaction of oleic acid with methanol with a low excess of methanol (3 equiv) proceeds faster on CMH−SO_3H catalysts having higher mesopore volumes. We also show that the properties of CMH−SO_3H catalysts can be tailored for the condensation reaction of 2-methylfuran and furfural, which form a bulky and hydrophobic product, **1**, in batch as well as continuous-flow reaction systems.

MATERIALS AND METHODS

Materials. Resorcinol (99.0%), formaldehyde (36.0 wt % aqueous solution stabilized by methanol), sodium carbonate (99.8%), 1 N HCl aq, 0.01 N NaOH aq, 0.01 N HCl aq, acetic acid (99.7%), ethanol (99.5%), oleic acid (99%), methanol (99%), 2-methylfuran (95%) were received from Wako Pure Chemical Industries, Ltd. Furfural (95%) was received from Sigma-Aldrich.

Synthesis of Catalysts. Catalysts were synthesized first in the form of a honeycomb-type monolith (CMH−SO_3H). For characterization and batch reaction experiments, these monoliths were crushed. For flow reaction experiments, as-prepared monoliths were used. A precursor RF resin was synthesized from a mixture of resorcinol (R), formaldehyde (F), sodium carbonate (C), and water (W) with a molar ratio among the four components being 1:2:0.02 or 0.005:61.[25,36] Typically, a mixture solution was charged to PP tubes that had been sealed at either end and heated at 303 K to allow the polycondensation reaction to proceed. After 20 h from the start of reaction, RF hydrogels were released from the PP molds and were washed with water. Then, each RF hydrogel was placed in a PP tube (13 mm i.d. × 125 mm), which was subsequently dipped into a liquid nitrogen bath at a rate of 60 mm h^{-1}. After the PP tube containing the frozen RF hydrogels were taken out of the liquid nitrogen bath, the hydrogels were thawed and aged in 20 mL of 1 N HCl aq in a glass vial at room temperature for 4 days. The resultant RF hydrogels were immersed in 10 times their volume of *tert*-butyl alcohol (*t*-BuOH) for 1 day to exchange the water included in their structure with *t*-BuOH. This washing process was repeated three times using fresh *t*-BuOH each time. The materials that had been washed with *t*-BuOH were freeze-dried at 263 K. The dried RF monoliths were pyrolyzed at 673 or 1273 K for 4 h in a tubular reactor in a nitrogen flow of 100 mL/min. The pyrolyzed materials were sulfonated using concentrated sulfuric acid at 353 K for 10 h and subsequently at 423 K for 5 h under a dry nitrogen atmosphere. The products were washed extensively with distilled and deionized water until no sulfate ions were detected in the water after washing. The washed materials were dried at 363 K in a convection oven.

The synthesized materials are denoted as CMH-*R*/*C* ratio-pyrolyzation temperature-SO_3H (if samples are sulfonated). For example, CMH-200-1273-SO_3H represents a catalyst prepared by resin synthesis at an *R*/*C* ratio of 200, followed by pyrolyzation at 1273 K and subsequently sulfonated.

Characterization. Morphology of the synthesized materials was characterized by a JEOL JSM-5410 scanning electron microscope (SEM, JEOL Japan Inc.), operating at an acceleration voltage of 30 kV and current of 15 μA. IR spectra of solid samples were collected in a transmission mode with a JASCO FT/IR-6100 Fourier transform spectrometer with a spectral resolution of 4 cm^{-1}. The sulfur contents in the synthesized catalysts were determined by elemental analysis using ICP. Boehm titration was performed according to the literature.[43−45] The standardization of the NaOH solutions was performed using potassium hydrogen phthalate as the primary standard, phenolphthalein as the indicator. Water vapor adsorption isotherms at 298 K were measured on an adsorption apparatus BELSORP-Max (BEL Japan, Inc.). Nitrogen adsorption/desorption isotherms at 77 K were measured on an adsorption apparatus BELSORP-mini II (BEL Japan, Inc.). The surface areas of the materials were calculated by the

DOI: 10.1021/acscatal.5b01022
ACS Catal. 2015, 5, 4951−4958

Braunner–Emmett–Teller (BET) method. The micropore and total pore volumes of the materials were estimated from adsorbed volumes at P/P_0 = 0.15 and 0.98, respectively. The mesopore size distributions were calculated by applying the Dollimore–Heal method to the adsorption isotherms.

Liquid-Phase Esterification Reaction of Acetic Acid with Ethanol and Oleic Acid with Methanol. Batch reactions were performed at 333 K in 3.5 mL sealed glass vials immersed in a water bath on an EYELA RCH-20L hot plate stirrer equipped with an ETS-D5 temperature controller. The vial reactors were initially loaded with the reaction mixture consisting of equimolar acetic acid and ethanol or a 1:3 molar ratio of oleic acid and methanol, sealed, and then immersed in the water bath at 333 K while each reaction mixture was stirred at 600 rpm. Solutions of reactants and an inert internal standard were allowed to reach 333 K prior to catalyst addition. Timer zero in the reaction was defined as the time when the catalyst was added. Before use in reactions, monolithic catalysts were ground (particle size <50 μm) and dried at 363 K for 2 h. Throughout the experiments, the reaction volume was kept constant at 3 mL. Sample aliquots (30 μL) were withdrawn from the reaction mixture using a micropipette, filtered, and analyzed using a Shimadzu GC-17A gas chromatograph equipped with a capillary column (Inert WAX-HT, GL Sciences, 30 m length, 0.25 mm diameter) coated with a 0.25 mm thick stationary phase (polyethylene glycol) and a flame ionization detector (FID). Initial rates were calculated from data collected at the conversion of the limiting reactant (acetic acid or oleic acid) <10%. When soluble acids were used as the catalyst, the reaction mixture was neutralized with $NaHCO_3$ prior to analysis.

Liquid-Phase Condensation Reaction of Furfural and 2-Methylfuran in a Batch Reactor. Condensation reactions were performed at 318 K using a procedure similar to that adopted for the esterification reactions. The vial reactors were initially loaded with the reaction mixture consisting of a 1:2.2 molar ratio of furfural and 2-methylfuran, sealed and then immersed in the water bath at 318 K while each reaction mixture was stirred at 600 rpm. Solutions of reactants and an inert internal standard were allowed to reach 318 K prior to catalyst addition. Timer zero in the reaction was defined as the time when the catalyst (0.01 mol equiv $-SO_3H$ group with respect to the limiting reagent), was added. Products were analyzed using a Shimadzu GC-17A gas chromatograph equipped with a capillary column (Inert WAX-HT, GL Sciences) and an FID.

Liquid-Phase Condensation Reaction of Furfural and 2-Methylfuran in a Flow Reaction System. A condensation reaction was also performed in a flow system at 318 K and atmospheric pressure. A monolithic CMH–SO_3H (50 mg) was sealed in a heat-shrinkable PFA tube, connected to inlet/outlet Teflon tubes, and held vertically in a thermostat bath at 318 K, as schematically shown in Figure S1 in the Supporting Information. A reaction mixture of 2-methylfuran and furfural in a 2.2:1 molar ratio was passed through the inlet Teflon tube and fed upward from the bottom of the catalyst at a liquid-hourly space velocity of 1.0 h^{-1}. A timer was started as the first drop of products came out of the top of the catalyst. The effluent was sampled and analyzed with a gas chromatography as carried out in the batch reactions.

RESULTS

Morphology and Porous Properties of Synthesized CMH and CMH–SO_3H. All synthesized catalysts were initially obtained in the monolithic form with honeycomb-like macropores (Figure 1, panels A and B). For characterization and

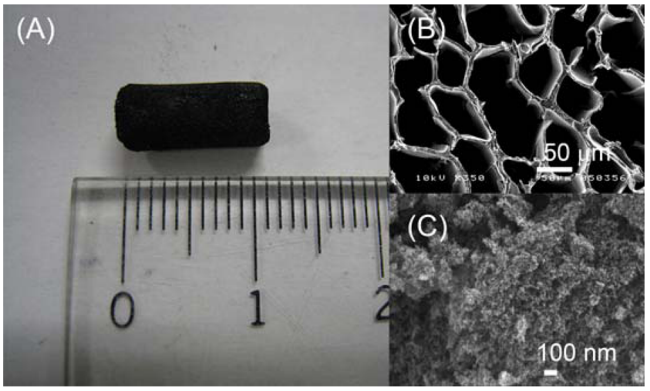

Figure 1. Synthesized CMH-200-1273-SO_3H: (A) photograph, (B) SEM image of the cross-sectional area of the monolith, (C) FE-SEM image characterizing the crushed sample.

batch reaction experiments, these monoliths were crushed, gently ground, and used. FE-SEM image characterizing a crushed catalyst (Figure 1, panel C) shows that the material consists of interconnected carbon nanoparticles <20 nm in diameter, which were derived from pyrolyzation of resorcinol–formaldehyde resin particles.

All samples exhibit type IV isotherms with hysteresis loops in N_2 adsorption/desorption data (Figure 2 for CMH–SO_3H catalysts and Figure S2 in the Supporting Information for unsulfonated CMH materials), indicating that the materials possess micro- and mesopores. Some major trends can be observed in the adsorption data (Table 1 and Figure 1). Increasing the R/C molar ratio from 50 to 200 increases the

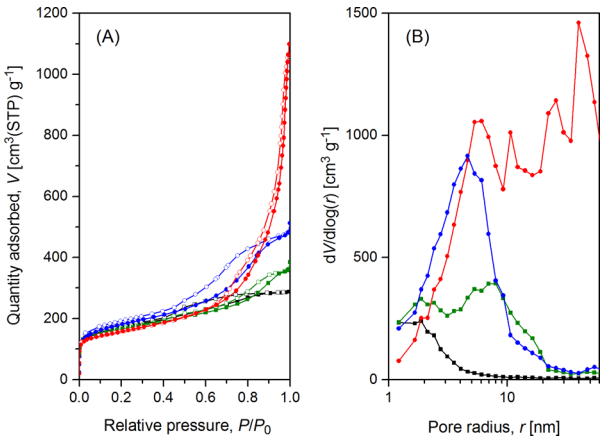

Figure 2. (A) Nitrogen gas adsorption/desorption isotherms characterizing CMH-50-673-SO_3H (■, □), CMH-50-1273-SO_3H (green ■, □), CMH-200-673-SO_3H (blue ●, ○), CMH-200-1273-SO_3H (red ●, ○). The open and closed symbols represent the data for adsorption and desorption branches, respectively. (B) Mesopore size distributions of CMH-50-673-SO_3H (■), CMH-50-1273-SO_3H (green ■), CMH-200-673-SO_3H (blue ●), CMH-200-673-SO_3H (red ●), as determined by applying the DH method to the adsorption branches.

DOI: 10.1021/acscatal.5b01022
ACS Catal. 2015, 5, 4951–4958

Table 1. Textural and Surface Properties of CMH and CMH−SO_3H

material	S_{BET}[a] [$m^2\ g^{-1}$]	V_{micro}[b] [$cm^3\ g^{-1}$]	V_{meso}[c] [$cm^3\ g^{-1}$]	V_{total}[d] [$cm^3\ g^{-1}$]	$x_{0.15}$[e] [%]	concentration of acid groups[f] [mmol g^{-1}]		
						$-SO_3H$	−COOH	−OH
CMH-50-673	667	0.28	0.15	0.43	28	n.a.[g]	0.08	0.80
CMH-50-773	686	0.25	0.14	0.39	9.6	n.a.	0.01	0.43
CMH-50-1273	731	0.30	0.51	0.81	1.6	n.a.	0.01	0.09
CMH-200-673	664	0.27	0.73	1.0	19	n.a.	0.07	0.60
CMH-200-1273	873	0.36	0.84	1.2	1.2	n.a.	0.01	0.29
CMH-50-673-SO_3H	618	0.25	0.20	0.45	58	0.97	0.49	0.82
CMH-50-773-SO_3H	673	0.28	0.17	0.45	41	0.91	0.16	0.49
CMH-50-1273-SO_3H	596	0.25	0.31	0.56	18	0.79	0.20	0.90
CMH-200-673-SO_3H	658	0.27	0.46	0.73	55	0.88	0.74	0.31
CMH-200-1273-SO_3H	570	0.23	1.5	1.7	30	0.62	0.48	0.64

[a]Surface area determined by BET method. [b]Micropore volume calculated from the uptake at P/P_0 = 0.15. [c]Mesopore volume calculated by subtracting V_{micro} from the uptake at P/P_0 = 0.98. [d]Total pore volume. [e]Ratio of water vapor uptake and nitrogen uptake at P/P_0 = 0.15. [f]Determined by Boehm method. [g]n.a. = not available.

mesopore volume (V_{meso}) and average mesopore size of unsulfonated CMH materials while retaining nearly the same micropore volume because a lower Na_2CO_3 concentration (higher R/C ratio) yields larger particles during sol gel synthesis,[22] which yields larger void spaces (mesopores and possibly small macropores) between them. Increasing the pyrolyzation temperature from 673 to 1273 K tends to increase V_{meso} of unsulfonated CMH materials probably because pyrolyzation at higher temperature results in the further decomposition of resin particles, yielding a higher pore volume. Sulfonated materials retained micromesoporosity but show slightly less V_{micro} and higher V_{meso}.

The PXRD data characterizing the synthesized catalysts (Figure S3 in the Supporting Information) show broad peaks at approximately 22 and 44°, which can be attributed to amorphous carbon composed of small graphene sheets oriented in a random fashion.

Surface Properties of Synthesized CMH and CMH−SO_3H. To characterize the type of surface oxygen-containing functional groups, synthesized materials were characterized by IR spectroscopy. IR spectra characterizing the unsulfonated CMH materials show bands typical of carbon gels (Figure 3): 1605 cm^{-1} for the aromatic ν(C═C), 1430 cm^{-1} for $\delta(CH_2)$ and the aromatic ν(C═C), and 1226 cm^{-1} for ν(O−C−O).[24]

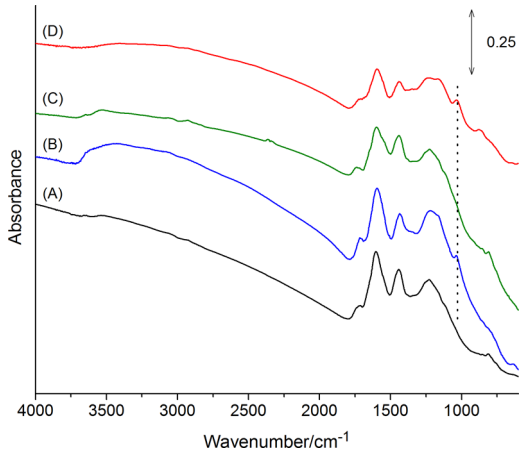

Figure 3. FT-IR spectra characterizing CMH-50-673 (A), CMH-50-673-SO_3H (B), CMH-200-673 (C), and CMH-200-673-SO_3H (D). The dotted line indicates the frequency corresponding to $\nu(SO_3^-)$.

The small band at 1730 cm^{-1} indicates the formation of a small amount of carboxyl groups presumably formed via slight oxidation of RF gels by air during synthesis. The samples prepared through pyrolyzation at 1273 K absorb IR light considerably, preventing meaningful characterization. The IR data characterizing the sulfonated catalysts show bands at 1032 cm^{-1}, which can be assigned to $\nu(SO_3^-)$ of hydrated $-SO_3H$ groups.[46,47]

Concentrations of these functional groups were determined by Boehm titration[19,43−45,48] and elemental analysis. Boehm titration uses several bases of various strengths (NaOH, Na_2CO_3, and $NaHCO_3$) to neutralize different surface oxygen functional groups. The weakest base, $NaHCO_3$, neutralizes strong acidic groups (i.e., $-SO_3H$) and weaker acid groups (i.e., carboxylic acid groups, −COOH). On the other hand, a stronger base, Na_2CO_3, neutralizes lactonic groups in addition to these acid groups. The strongest base, NaOH, neutralizes phenolic groups and carboxylic lactonic groups as well. Thus, the concentration of each group of acidic surface functional groups can be determined by the difference between the uptake of each base. In the present work, a combined analysis of titration using NaOH and $NaHCO_3$ and elemental sulfur analysis was used to quantify sulfonic acid groups, carboxylic acid groups, and hydroxyl and lactonic groups. The data obtained by Boehm titration for uncalcined CMH materials show a gradual decrease in the concentration of −OH groups by increasing pyrolyzation temperature as expected (Table 1). The data also show a small amount of −COOH groups present in the materials pyrolyzed at 673 K, consistent with the IR spectroscopy data. After sulfonation, 0.6−1 mmol g^{-1} of $-SO_3H$ groups was introduced into CMH materials with a significantly increased concentration of −COOH groups. As shown by the catalysis experiments, the acid groups other than $-SO_3H$ groups exhibit negligible contributions toward catalysis probably because of their weak acidity.

To quantify the degree of the hydrophobicity of the surface of the synthesized materials, we measured water vapor uptake at 298 K and compared the ratio of water vapor uptake volume (V_{H_2O}) and nitrogen uptake volume (V_{N_2}) measured at relative pressure P/P_0 = 0.15. This value, which is denoted as $x_{0.15}$, serves as a good metric to analyze the surface hydrophobicity; a lower $x_{0.15}$ value indicates that the surface is more hydrophobic. This method has been used in analyzing the surface properties of microporous materials such as zeolites[49,50] but was found to

DOI: 10.1021/acscatal.5b01022
ACS Catal. 2015, 5, 4951−4958

be applicable to micromesoporous carbons. Table 1 shows that $x_{0.15}$ is influenced most by the pyrolyzation temperature as expected, giving lower values as the pyrolyzation temperature was raised. CMH-50-1273 and -200-1273 show significantly low $x_{0.15}$, as typically found for other highly hydrophobic adsorbents.[25] Sulfonation of CMH materials increased the surface hydrophilicity as the concentrations of oxygen-containing surface functional groups increased (Table 1).

Liquid-Phase Esterification Reactions. To test the catalytic performance of synthesized catalysts, the esterification of acetic acid with ethanol was conducted in a batch reactor using crushed catalysts. The reaction proceeded at nearly the same rate for all CMH−SO_3H catalysts (Figure 4 and Table 2).

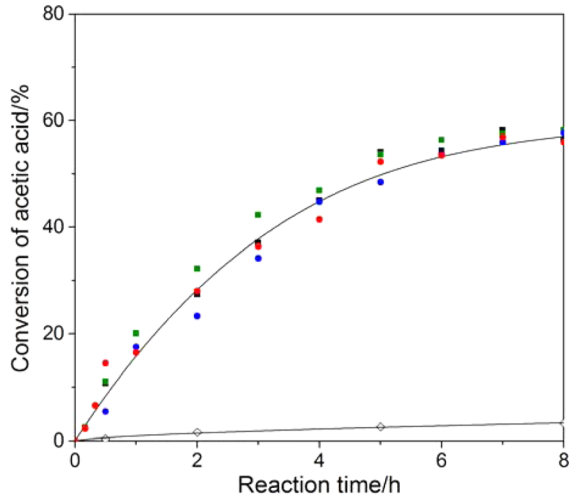

Figure 4. Esterification of acetic acid with ethanol in a batch reactor using crushed CMH-50-673-SO_3H (■), CMH-50-1273-SO_3H (green ■), CMH-200-673-SO_3H (blue ●), or CMH-200-1273-SO_3H (red ●). Acetic acid (25 mmol), ethanol (25 mmol), catalyst −SO_3H sites (75 μmol). Reaction temperature = 333 K. The data shown by (◊) symbol was obtained without catalyst addition.

Table 2. Esterification of Acetic Acid with Ethanol in a Batch Reactor[a]

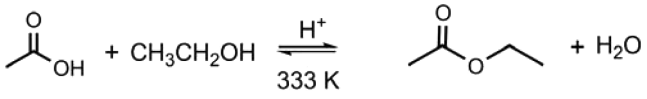

catalysts	initial TOF[b] [s^{-1}]
CMH-50-673-SO_3H	0.023
CMH-50-1273-SO_3H	0.025
CMH-200-673-SO_3H	0.022
CMH-200-1273-SO_3H	0.024

[a]Conditions: acetic acid (25 mmol), ethanol (25 mmol), catalyst −SO_3H sites (75 μmol). [b]Calculated by the limiting reagent, acetic acid, conversion <10%. Experimental error <15%.

A reaction experiment without an added catalyst shows a low conversion (1.6% in 2 h). Turnover frequencies (TOFs) of all catalysts, which were calculated per −SO_3H group for the acetic acid conversion <10%, gave ∼0.02 s^{-1} regardless of their different surface hydrophobicity and pore structure.

To evaluate the accessibility of reactants to the active sites of CMH−SO_3H catalysts, selective poisoning experiments were conducted using NaCl. A known amount of a CMH−SO_3H catalyst was added to water including a known amount of NaCl, stirred at ambient temperature for 24 h to let the NaCl equilibrate with the active sites, separated, and dried. The reaction data using the partially poisoned (Figure S3 in the Supporting Information) show that the rate decreases linearly with increasing the degree of poisoning, which is expressed by the (mol of NaCl added)/(mol of initial −SO_3H) ratio, extrapolating to nearly zero at a degree of poisoning of 1. Thus, the results indicate that the reaction proceeds at a single site (−SO_3H), and essentially all −SO_3H groups can be accessed by reactants. The data also show that other weak acid groups made a negligible contribution to catalysis, as had been expected. It is generally accepted that the esterification reaction occurs via the rate-determining step of the nucleophilic attack of the alcohol on the protonated carbonyl group of the carboxylic acid. Thus, strong acid appears to be effective to form a high concentration of protonated carbonyl groups.

To investigate the catalytic performance of the CMH−SO_3H further, esterification of oleic acid with methanol was conducted at 333 K using crushed catalysts. In sharp contrast to the results obtained in the esterification reaction of acetic acid with ethanol, the catalysts exhibit a variation of activities, showing that catalysts with larger mesopores exhibit higher rates (Figure 5 and Table 3). Activation energies for CMH-50-

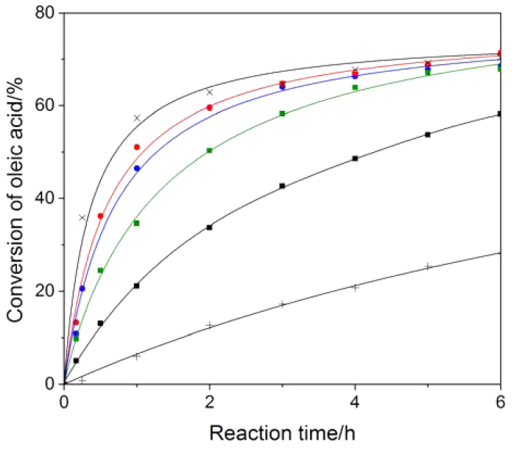

Figure 5. Esterification of oleic acid with methanol in a batch reactor using crushed CMH-50-673-SO_3H (■), CMH-50-1273-SO_3H (green ■), CMH-200-673-SO_3H (blue ●), or CMH-200-1273-SO_3H (red ●).The data shown in (×) and (+) represent those for *p*-TSA and Amberyst-15, respectively. Oleic acid (6 mmol), methanol (18 mmol), catalyst −SO_3H sites (30 μmol). Reaction temperature = 333 K.

1273-SO_3H and CMH-200-1273-SO_3H are both approximately 40 kJ mol^{-1} (Table 3 and Figure S5 in the Supporting Information), which are similar to that for *p*-TSA within experimental errors.

The reusability of CMH-200-1273-SO_3H was tested in a batch reaction experiment because some literature has reported deactivation of sulfonic-acid-containing carbons prepared from sugars.[12,51,52] After each cycle, the catalyst was recovered by centrifugation at 3000 rpm, washed with methanol at ambient temperature, dried at 363 K overnight. After the dried catalyst was weighed again, it was used in the next cycle. The results show nearly the same initial TOF for the 4 cycles within the error of the experiment (Figure S6 in the Supporting Information), showing the good reusability of the catalyst.

The reaction proceeded at a much lower rate for Amberlyst-15 probably because it did not swell enough under the

DOI: 10.1021/acscatal.5b01022
ACS Catal. 2015, 5, 4951−4958

Table 3. Esterification of Oleic Acid with Methanol in a Batch Reactor[a]

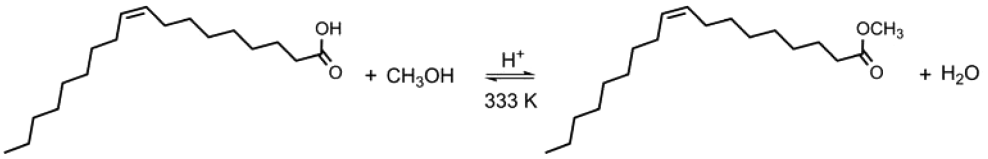

catalysts	apparent initial TOF[b] [s^{-1}]	activation energy [kJ mol^{-1}]
CMH-50-673-SO_3H	0.017	52 ± 5 (293–313 K)[c]
		17 ± 5 (313–333 K)[c]
CMH-50-1273-SO_3H	0.032	49 ± 2
CMH-200-673-SO_3H	0.040	37 ± 3
CMH-200-1273-SO_3H	0.042	45 ± 4
Amberlyst-15	0.0019	41 ± 11
p-TSA	0.064	40 ± 5

[a]Conditions: oleic acid (6 mmol), methanol (18 mmol), catalyst −SO_3H sites (30 μmol). [b]Calculated by the limiting reagent, oleic acid, conversion <10%. Experimental error <15%. [c]Data can be fitted by two different lines depending on the temperature range (Figure S5 in the Supporting Information).

methanol concentration used in the present conditions. These results show promising performance for CMH−SO_3H in the esterification of bulky substrates.

Condensation of 2-Methylfuran with Furfural in a Batch Reactor. Catalytic performance of CMH catalysts was further evaluated in the condensation of furfural and 2-methylfuran to form **1**. For comparison, experiments were also conducted using Amberlyst-15 and *p*-TSA. As expected, the synthesized catalysts having surfaces with higher hydrophobicity and larger mesopore volumes showed higher catalytic activities as shown in Figure 6 and Table 4. In particular, CMH-200-1273-SO_3H exhibits a high TOF, only 20% less than that of *p*-TSA. Notably, three of the CMH−SO_3H catalysts exhibit much higher selectivity than Amberlyst-15 (Table 3). The relatively low selectivity for the other CMH−SO_3H (CMH-50-673-SO_3H) may be explained by its low V_{meso} and smaller mesopore size, preventing the efficient formation of **1**. CMH-200-1273-SO_3H, which exhibits the highest reaction rate among the CMH catalysts, maintained a high selectivity (>90%) throughout the course of the reaction, suggesting promising catalytic applications of CMH−SO_3H catalysts to this class of reactions.

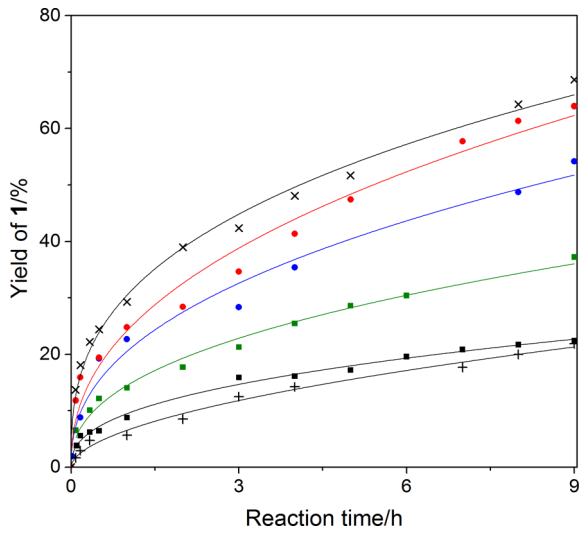

Figure 6. Condensation of furfural with 2-methylfuran in a batch reactor using crushed CMH-50-673-SO_3H (■), CMH-50-1273-SO_3H (green ■), CMH-200-673-SO_3H (blue ●), or CMH-200-1273-SO_3H (red ●). The data shown in (×) and (+) represents those for *p*-TSA and Amberlyst-15, respectively. Furfural (4 mmol), 2-methylfuran (8.8 mmol), catalyst −SO_3H sites (40 μmol). Reaction temperature = 318 K.

Table 4. Condensation of Furfural with 2-Methylfuran to Produce 1 in a Batch Reactor[a]

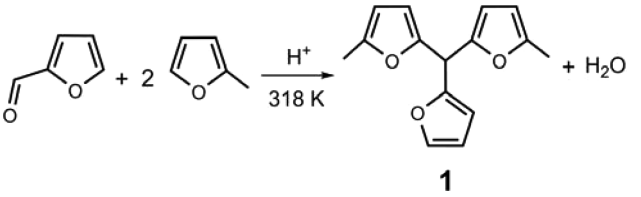

1

catalysts	apparent initial TOF[b] [s^{-1}]	furfural conversion[c] [%]	yield of **1**[c] [%]	selectivity[c] [%]
CMH-50-673-SO_3H	0.010	32	22	69
CMH-50-1273-SO_3H	0.022	39	37	95
CMH-200-673-SO_3H	0.034	59	54	92
CMH-200-1273-SO_3H	0.041	71	64	90
Amberlyst-15	0.0050	29	22	76
p-TSA	0.052	77	69	90

[a]Conditions: furfural (4 mmol), 2-methylfuran (8.8 mmol), catalyst −SO_3H sites (40 μmol). [b]Calculated by the limiting reagent conversion <10%. [c]Values at t = 9 h.

Condensation of 2-Methylfuran with Furfural in a Continuous-Flow Reaction System. To investigate the potential of CMH−SO_3H for application to continuous-flow reaction systems, the condensation reaction was performed using a monolithic CMH−SO_3H. Because a CMH-type catalyst consists of a large number of nearly straight channels in the micrometer range, it mimics a bundle of capillaries, functioning as a microreactor-type catalyst.[36] Thus, a CMH−SO_3H was directly used as a monolithic catalyst in this experiment. The catalyst was found to exhibit stable activity for >24 h, yielding **1** at 23 ± 1% under the present conditions (Figure 7).

DISCUSSION

Surface hydrophobicity/hydrophilicity and accessibility of active sites are important factors when designing solid acid catalysts, especially for liquid-phase reactions. When reactants

DOI: 10.1021/acscatal.5b01022
ACS Catal. 2015, 5, 4951−4958

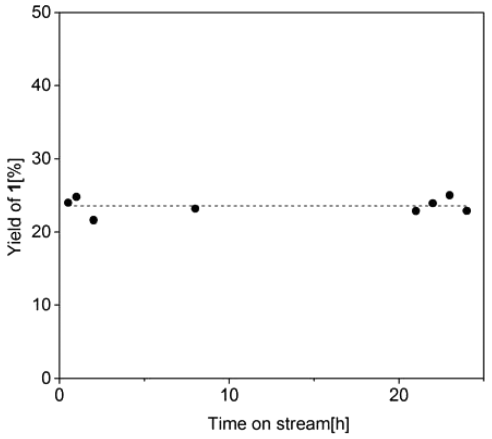

Figure 7. Condensation of furfural with 2-methylfuran using CMH-200-1273-SO_3H in a continuous-flow system. Liquid hourly space velocity (LHSV) = 1.0 h^{-1}. Feed: a mixture of furfural and 2-methylfuran in a 1:2.2 ratio. Reaction temperature = 318 K.

consist of highly polar substrates (e.g., short-chain alcohols and acids) or a large excess of polar substrates is used, solid acid catalysts that have highly hydrophilic surfaces can swell, and the active sites initially embedded deep inside them become accessible. However, minimizing the amount of excess polar substrates is advantageous for reducing the energy input required for downstream separation units, which require catalysts whose active sites can be accessible even in a relatively hydrophobic media. Moreover, swelling of catalyst particles are undesirable for application to flow reaction systems using a fixed-bed reactor because it may cause bursting of the reactor.[7] Furthermore, when substrates consist of hydrophobic molecules, particularly large bulky molecules, solid acid catalysts having hydrophobic surfaces and large mesopores are preferred.

This work demonstrate the tunability of surface hydrophobicity/hydrophilicity and pore structure of carbon-based acid catalysts for typical liquid-phase reactions. Our results show that solid acid catalysts derived from phenolic resins can be readily tailored for reactions involving highly polar small molecules (i.e., acetic acid + ethanol), more hydrophobic and bulky molecules (i.e., oleic acid + methanol, 3 equiv excess of methanol), and bulky hydrophobic molecules (i.e., condensation of furfural with 2-methylfuran).

Our data show that all CMH−SO_3H catalysts exhibit nearly the same catalytic activity in the esterification of acetic acid with ethanol regardless of the difference of their mesopore size and volume probably because of the smallness of the substrates. A comparison with some literature data[9,12,16,53−55] (Table S1 in the Supporting Information) show that TOFs for CMH−SO_3H catalysts are similar or in the same order of magnitude to those containing sulfonic-acid containing resins or carbons. The poisoning experiment confirms the high accessibility of strong acid sites of CMH−SO_3H catalysts for this reaction. On the other hand, when a more bulky oleic acid is used with a polar substrate (methanol) in the esterification reaction, the catalysts containing a large volume of mesopores (>0.4 $cm^3\ g^{-1}$), CMH-200-673-SO_3H and -1273-SO_3H, exhibit higher catalytic performance than other catalysts. Activation energies of CMH-200-1273-SO_3H are approximately 40 kJ mol^{-1}, similar to that of *p*-TSA within the error of experiments. Thus, we infer that −SO_3H groups in these CMH−SO_3H catalysts function similarly to those in *p*-TSA. In contrast, an Arrhenius plot for CMH-50-673-SO_3H appears to be bent and can be only fitted with two lines depending on the temperature range (Figure S5). The low activation energy (17 ± 5) in the higher temperature range suggests severe mass transport limitation.[56] To confirm whether the reaction using CMH-200-1273-SO_3H proceeded in the kinetically controlled regime, the Weisz−Prater modulus was calculated (see the Supporting Information).[57,58] The results confirm negligible intraparticle mass transfer resistance. For this esterification reaction, the difference in the surface hydrophobicity as characterized by $x_{0.15}$ does not appear significantly affect catalytic performance under the present conditions. However, when both reactants and products are hydrophobic and the size of the product is large as in the condensation of furanic compounds, both hydrophobicity and mesopore volume influence the catalytic performance significantly. The reaction proceeded faster on catalysts having more hydrophobic surfaces and a large mesopore volume. The rates of CMH−SO_3H are much higher than that for Amberlyst-15. Furthermore, our data show that the reaction can also be performed in a continuous-flow system using a monolithic form of a CMH−SO_3H catalyst.

CONCLUSIONS

In conclusion, we have shown the high tunability of pore and surface properties of carbon-based acid catalysts derived from phenolic resins for several liquid-phase reactions. The effects of pore and surface properties are most manifested in the condensation reaction of furfural and 2-methylfuran, which requires large pores (>4 nm) and relatively hydrophobic surfaces. CMH-200-1273-SO_3H can catalyze this reaction at a much higher rate and selectivity than Amberlyst-15 in a batch reaction system and also exhibits stable catalytic performance in a flow reaction system. The results suggest that further tuning to increase surface hydrophobicity and mesopore size and volume may be effective for this reaction as well as similar types of reactions. On the other hand, pore properties of CMH−SO_3H seem to play an important role in the esterification of oleic acid with methanol for which both CMH-200-673-SO_3H and CMH-200-1273-SO_3H exhibit high catalytic activities. Further tuning to facilitate mass transfer of substrates may be effective to make the catalytic performance of CMH−SO_3H catalysts to approach that of *p*-TSA. In contrast to these reactions, all CMH−SO_3H exhibit similar activity in the esterification of acetic acid with ethanol. Thus, the results suggest that this reaction may be a good model reaction to assess the activity of acid sites of various carbon-based acid catalysts without the influence of mass transfer of substrates.

Our work suggests that carbon materials derived from phenolic resins may be applied to various acid-catalyzed liquid-phase reactions. Further precise tuning will expand the range of reactions that this class of catalysts can catalyze.

ASSOCIATED CONTENT

Supporting Information

The Supporting Information is available free of charge on the ACS Publications website at DOI: 10.1021/acscatal.5b01022.

List of literature data for esterification reactions. Schematic for the experimental setup for a flow reaction system. Nitrogen gas adsorption/desorption isotherms and pore size distributions for CMH materials. PXRD data characterizing CMH−SO_3H catalysts. Data from poisoning experiments. Arrhenius plots. Data from the reusability test of CMH-200-1273-SO_3H in the ester-

DOI: 10.1021/acscatal.5b01022
ACS Catal. 2015, 5, 4951−4958

ification of oleic acid with methanol. Analysis of the reaction data by the Weisz−Prater criterion (PDF)

AUTHOR INFORMATION

Corresponding Author

*E-mail: iogino@eng.hokudai.ac.jp. Tel: +81 (11) 706-6591.

Notes

The authors declare no competing financial interest.

REFERENCES

(1) Corma, A. *Chem. Rev.* **1997**, *97*, 2373−2420.
(2) Chakrabarti, A.; Sharma, M. M. *React. Polym.* **1993**, *20*, 1−45.
(3) Tanabe, K.; Hölderich, W. F. *Appl. Catal., A* **1999**, *181*, 399−434.
(4) Okuhara, T. *Chem. Rev.* **2002**, *102*, 3641−3665.
(5) Tanabe, K. *Catal. Today* **2003**, *78*, 65−77.
(6) Arata, K.; Matsuhashi, H.; Hino, M.; Nakamura, H. *Catal. Today* **2003**, *81*, 17−30.
(7) Gates, B. C. In *Handbook of Heterogeneous Catalysis*, 2nd ed.; Ertl, G., Knözinger, H., Schüth, F., Weitkamp, J., Eds.; Verlag Chemie: Weinheim, Germany, 2008; Vol. *1*, pp 278−285.
(8) Bruno, J. E.; Dooley, K. M. *Appl. Catal., A* **2015**, *497*, 176−183.
(9) Hara, M.; Yoshida, T.; Takagaki, A.; Takata, T.; Kondo, J. N.; Hayashi, S.; Domen, K. *Angew. Chem., Int. Ed.* **2004**, *43*, 2955−2958.
(10) Toda, M.; Takagaki, A.; Okamura, M.; Kondo, J. N.; Hayashi, S.; Domen, K.; Hara, M. *Nature* **2005**, *438*, 178−178.
(11) Suganuma, S.; Nakajima, K.; Kitano, M.; Yamaguchi, D.; Kato, H.; Hayashi, S.; Hara, M. *J. Am. Chem. Soc.* **2008**, *130*, 12787−12793.
(12) Mo, X.; Lopez, D. E.; Suwannakarn, K.; Liu, Y.; Lotero, E.; Goodwin, J. G., Jr.; Lu, C. Q. *J. Catal.* **2008**, *254*, 332−338.
(13) Mo, X. H.; Lotero, E.; Lu, C. Q.; Liu, Y. J.; Goodwin, J. G. *Catal. Lett.* **2008**, *123*, 1−6.
(14) Kitano, M.; Arai, K.; Kodama, A.; Kousaka, T.; Nakajima, K.; Hayashi, S.; Hara, M. *Catal. Lett.* **2009**, *131*, 242−249.
(15) Onda, A.; Ochi, T.; Yanagisawa, K. *Top. Catal.* **2009**, *52*, 801−807.
(16) Hara, M. *Top. Catal.* **2010**, *53*, 805−810.
(17) Fukuhara, K.; Nakajima, K.; Kitano, M.; Kato, H.; Hayashi, S.; Hara, M. *ChemSusChem* **2011**, *4*, 778−784.
(18) Nakajima, K.; Hara, M. *ACS Catal.* **2012**, *2*, 1296−1304.
(19) Kobayashi, H.; Yabushita, M.; Komanoya, T.; Hara, K.; Fujita, I.; Fukuoka, A. *ACS Catal.* **2013**, *3*, 581−587.
(20) Chung, P.-W.; Charmot, A.; Olatunji-Ojo, O. A.; Durkin, K. A.; Katz, A. *ACS Catal.* **2014**, *4*, 302−310.
(21) Pekala, R. W. *J. Mater. Sci.* **1989**, *24*, 3221−3227.
(22) Pekala, R. W.; Alviso, C. T.; Kong, F. M.; Hulsey, S. S. *J. Non-Cryst. Solids* **1992**, *145*, 90−98.
(23) Al-Muhtaseb, S. A.; Ritter, J. A. *Adv. Mater.* **2003**, *15*, 101−114.
(24) Stein, A.; Wang, Z. Y.; Fierke, M. A. *Adv. Mater.* **2009**, *21*, 265−293.
(25) Ogino, I.; Kazuki, S.; Mukai, S. R. *J. Phys. Chem. C* **2014**, *118*, 6866−6872.
(26) Rolison, D. R. *Science* **2003**, *299*, 1698−1701.
(27) Tsuchiya, T.; Mori, T.; Iwamura, S.; Ogino, I.; Mukai, S. R. *Carbon* **2014**, *76*, 240−249.
(28) Hanzawa, Y.; Kaneko, K.; Pekala, R. W.; Dresselhaus, M. S. *Langmuir* **1996**, *12*, 6167−6169.
(29) Mukai, S. R.; Nishihara, H.; Tamon, H. *Chem. Commun. (Cambridge, U. K.)* **2004**, 874−875.
(30) Nishihara, H.; Mukai, S. R.; Tamon, H. *Carbon* **2004**, *42*, 899−901.
(31) Mukai, S. R.; Nishihara, H.; Yoshida, T.; Taniguchi, K.; Tamon, H. *Carbon* **2005**, *43*, 1563−1565.
(32) Mukai, S. R.; Tamitsuji, C.; Nishihara, H.; Tamon, H. *Carbon* **2005**, *43*, 2628−2630.
(33) Inagaki, M.; Qiu, J.; Guo, Q. *Carbon* **2015**, *87*, 128−152.
(34) Davis, R. J. In *Catalysis for the Conversion of Biomass and Its Derivatives*; Behrens, M., Datye, A. K., Eds.; Max Planck Research Library for the History and Development of Knowledge: Berlin, 2013; pp 255−291.
(35) Lopez-Ruiz, J. A.; Davis, R. J. *Green Chem.* **2014**, *16*, 683−694.
(36) Murakami, K.; Satoh, Y.; Ogino, I.; Mukai, S. R. *Ind. Eng. Chem. Res.* **2013**, *52*, 15372−15376.
(37) Corma, A.; de la Torre, O.; Renz, M. *Energy Environ. Sci.* **2012**, *5*, 6328−6344.
(38) Corma, A.; de la Torre, O.; Renz, M.; Villandier, N. *Angew. Chem., Int. Ed.* **2011**, *50*, 2375−2378.
(39) Balakrishnan, M.; Sacia, E. R.; Bell, A. T. *ChemSusChem* **2014**, *7*, 1078−1085.
(40) Yati, I.; Yeom, M.; Choi, J.-W.; Choo, H.; Suh, D. J.; Ha, J.-M. *Appl. Catal., A* **2015**, *495*, 200−205.
(41) Teo, H.; Saha, B. *J. Catal.* **2004**, *228*, 174−182.
(42) Harmer, M. A.; Sun, Q. *Appl. Catal., A* **2001**, *221*, 45−62.
(43) Boehm, H. P. *Carbon* **1994**, *32*, 759−769.
(44) Goertzen, S. L.; Thériault, K. D.; Oickle, A. M.; Tarasuk, A. C.; Andreas, H. A. *Carbon* **2010**, *48*, 1252−1261.
(45) Oickle, A. M.; Goertzen, S. L.; Hopper, K. R.; Abdalla, Y. O.; Andreas, H. A. *Carbon* **2010**, *48*, 3313−3322.
(46) Krasovskii, A. N.; Kalnin'sh, K. K. *J. Appl. Spectrosc.* **1977**, *26*, 745−749.
(47) Tipson, R. S. *J. Am. Chem. Soc.* **1952**, *74*, 1354−1354.
(48) Boehm, H. P. *Carbon* **2002**, *40*, 145−149.
(49) Thommes, M.; Mitchell, S.; Pérez-Ramírez, J. *J. Phys. Chem. C* **2012**, *116*, 18816−18823.
(50) Gounder, R.; Davis, M. E. *AIChE J.* **2013**, *59*, 3349−3358.
(51) Roldán, L.; Pires, E.; Fraile, J. M.; García-Bordejé, E. *Catal. Today* **2015**, *249*, 153.
(52) Fraile, J. M.; García-Bordejé, E.; Roldán, L. *J. Catal.* **2012**, *289*, 73.
(53) Fraile, J. M.; García-Bordejé, E.; Pires, E.; Roldán, L. *J. Catal.* **2015**, *324*, 107−118.
(54) Peters, T. A.; Benes, N. E.; Holmen, A.; Keurentjes, J. T. F. *Appl. Catal., A* **2006**, *297*, 182−188.
(55) Constantino, D. S. M.; Pereira, C. S. M.; Faria, R. P. V.; Ferreira, A. F. P.; Loureiro, J. M.; Rodrigues, A. E. *AIChE J.* **2015**, *61*, 1263−1274.
(56) Davis, M. E.; Davis, R. J. *Fundamentals of Chemical Reaction Engineering*, International ed.; McGraw-Hill: Boston, 2003.
(57) Weisz, P. B.; Prater, C. D. In *Advances in Catalysis*; Frankenburg, W.G., Komarewsky, V. I., Rideal, E. K., Eds.; Elsevier: Amsterdam, 1954; Vol. *6*, pp 143−196.
(58) Mears, D. E. *Ind. Eng. Chem. Process Des. Dev.* **1971**, *10*, 541−547.

DOI: 10.1021/acscatal.5b01022
ACS Catal. 2015, 5, 4951−4958